Proceedings of the ASME 2012 International Design Engineering Technical Conferences & Computers and Information in Engineering Conference
IDETC/CIE 2012
August 12-15, 2012, Chicago, IL, USA

DETC2012-70220

IMPROVING THE PERFORMANCE OF A PIEZOELECTRIC ENERGY HARVESTER USING A TIP SPRING-MASS SYSTEM

Yang Zhu* **Oumar Barry** **Weijiun Su** **Jean Zu**
Department of Mechanical and Industrial Engineering,
University of Toronto
Toronto, Ontario, Canada M5S3G8

ABSTRACT

Vibration-based energy harvesting using piezoelectric materials has gained considerable attention over the past decade. Currently, most piezoelectric energy harvesters (PEHs) are single resonance frequency based. The performance of a single-resonance PEH is often limited to only one resonance frequency. This paper discusses the possibility of improving the performance of a bimorph PEH by tuning the PEH using a spring-mass system attached to the bimorph's free end. Through adding the spring-mass system, the PEH's resonance frequency can be tuned to match the ambient vibration frequency, and its voltage/power-generating capability can be improved. An electromechanical model of the PEH is derived based on the Lagrange multiplier method. The model is then used in a harmonic base excitation case study, and the coupled electromechanical outputs are discussed. Simulation results show that the spring-mass attachment can create two resonant frequencies, making the PEH capable of working efficiently at two different frequencies in a low-frequency level. It is also shown that by properly selecting the spring stiffness and the mass, the voltage and power output of the PEH can be greatly increased as compared to a single bimorph without the spring-mass system.

INTRODUCTION

Vibration-based energy harvesting is a promising technology for providing power supplies to small-scale electronic devices. Piezoelectric materials are most often used in the research and design of vibration-based energy harvesters [1]. By converting ambient vibration energy to electrical energy, piezoelectric energy harvesters (PEHs) provide a promising way for developing self-powered electronic devices such as wireless sensor networks.

A conventional PEH is a cantilever with one or two piezoceramic layers, also known as a unimorph or bimorph. The cantilevered energy harvester is often located on a vibrating base. Due to the piezoelectric effect [2], the dynamic bending strain induced in the piezoceramic layer(s) causes an alternating electric potential difference between the electrodes covering the piezoceramic layer(s). Major limitations in the conventional PEH include its relatively small power output and its dependence on a single resonance frequency. In practical cases, vibration levels can be very low (<1 m/s^2) at frequencies that are less than 60 Hz [3]. Therefore, it is very important to tune the resonant frequency of a single-resonance PEH so that it matches the frequency of the ambient vibration. Methods including passive tuning and active tuning [4] have been used to tune the single-resonance energy harvesters. The active mode requires continuous power input for resonance tuning whereas the passive mode needs intermittent power input. Various transducer mechanisms have been used for the resonance tuning of vibration-based energy harvesters, such as proof mass method [5, 6], magnetic force method [7], pre-straining method [8,9], and so forth. The aim of this paper is to use a tip spring-mass system to tune a cantilevered PEH, thus to create double resonance frequencies and improve the PEH's power generating ability. It is shown that the tip spring-mass system not only acts as a tuning component, but also greatly increases the PEH's power output at its lower resonance frequency. Moreover, from the results of the parametric study, it is shown that by properly selecting the mass and spring stiffness, the tip spring-mass system can assist the PEH to work more efficiently at both low and high resonance frequencies.

ELECTROMECHANICAL MODEL

This section presents the system configuration and mathematical model of the proposed PEH. As shown in Fig. 1, the PEH consists of one bimorph and a spring-mass system attached at the bimorph's free end. The bimorph is made of a cantilever sandwiched by two piezoceramic layers. When a

* Corresponding author: young@mie.utoronto.ca

harmonic base excitation is applied, the bending of the piezoceramic layers results in a voltage/power across a resistive load due to piezoelectric effects. In order to derive the expressions for the electromechanical responses of the system, it is necessary to first formulate the system's equation of motion. To this end the energy method and the Lagrange multipliers method are used.

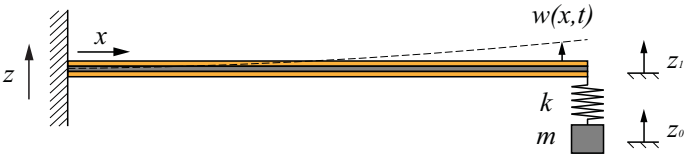

Figure 1. System configuration of the piezoelectric energy harvester with a tip spring-mass system

The kinetic energy within each layer is distributed along the length of the beam. Assuming the piezoelectric layer covers the whole length of the cantilever, the kinetic energy for the substrate and the piezoelectric layers are

$$T_s = \frac{1}{2}\rho_s A_s \int_0^L [\dot{w}(x,t) + \dot{z}(t)]^2 dx \quad (1)$$

$$T_p = \frac{1}{2}\rho_p A_p \int_0^L [\dot{w}(x,t) + \dot{z}(t)]^2 dx \quad (2)$$

where ρ_s and ρ_p are the material density of the substrate and piezoelectric layer, A_s and A_p are the cross-sectional area of the substrate and two piezoelectric layers, L is the length of the beam, $w(x,t)$ is the transverse deflection of the bimorph, $z(t)$ is the base excitation. In addition, the mass m_e in the tip spring-mass system has kinetic energy

$$T_m = \frac{1}{2} m_e [\dot{z}_0(t) + \dot{z}(t)]^2 \quad (3)$$

where $z_0(t)$ is the displacement of the mass.

The potential energy of the system comes from the bimorph and the spring. The potential energy of the bimorph is the same as the work done in deforming the bimorph, and can be obtained using Euler-Bernoulli beam theory. For the substrate, the potential energy is

$$U_s = \frac{1}{2} E_s I_s \int_0^L w''(x,t)^2 dx \quad (4)$$

For the piezoelectric layer, it has not only an elastic potential due to bending, but also an electrical potential due to piezoelectric effect. Assuming a series connection of the piezoelectric layers is used, the potential energy of the two piezoelectric layers can be expressed as

$$U_p = E_p I_p \int_0^L w''(x,t)^2 dx + \vartheta v(t) - \frac{1}{4} C_p v(t)^2 \quad (5)$$

where b is the width of the bimorph, h_s and h_s are the thickness of the substrate and the piezoelectric layers, E_s and E_p are the Young' modulus for the substrate and the piezoelectric material, $I_s = bh_s^3/12$ is the moment of inertia for the substrate and $I_p = bh_p(4h_p^2 + 6h_p h_s + 3h_s^2)/12$ is the moment of inertia for the piezoelectric layers, e_{31} is the piezoelectric coupling coefficient, $v(t)$ is the voltage generated across the piezoelectric layers, $\vartheta_1 = -e_{31} b(h_p + h_s) w_1'(L)/2$ is the electromechanical coupling term, $C_p = b\varepsilon_{33}^S L / h_p$ is the effective capacitance through one piezoelectric layer. Moreover, for the spring the potential energy is

$$U_k = \frac{1}{2} k_e [z_1(t) - z_0(t)]^2 \quad (6)$$

where k_e is the stiffness of the spring, $z_1 = w(L,t)$ is the tip displacement of the bimorph. Therefore, the Lagrangian equation for the system is the difference in kinetic energy and potential energy

$$L = T_s + T_p + T_m - U_s - U_p - U_k \quad (7)$$

The method of separation [10] is used here to discretize the Lagrangian equation. The transverse displacement of the beam at point x is expressed as

$$w(x,t) = \sum_{i=1}^{\infty} w_i(x)\eta_i(t) \quad (8)$$

where $w_i(x)$ and $\eta_i(t)$ are the mode shape and the modal coordinate of the beam for the i-th mode. The mode shape function can be expressed as

$$w_i(x) = C_1 \cos\beta x + C_2 \sin\beta x + C_3 \cosh\beta x + C_4 \sinh\beta x \quad (9)$$

where β can be found from the system's frequency equation, which will be discussed later. The constants C_i are obtained using the boundary conditions

$$w(0,t) = 0, \quad \left.\frac{\partial w(x,t)}{\partial x}\right|_{x=0} = 0 \quad (10)$$

$$\left.\frac{\partial^2 w(x,t)}{\partial x^2}\right|_{x=l} = 0, \; EI \left.\frac{\partial^3 w(x,t)}{\partial x^3}\right|_{x=l} = m_e \ddot{z}_0 \quad (11)$$

where $EI = 2E_p I_p + E_s I_s$ is the bending stiffness of the beam. Note that the motion of the mass is related to the tip motion of the beam as

$$m_e \ddot{z}_0 + k_e(z_0 - z_1) = 0 \quad (12)$$

By evaluating Eq. (10) ~ (12) in Eq. (9), the mode shape function is normalized to

$$w_i(x) = \frac{1}{\sqrt{mL}}[\cos\beta_i x - \cosh\beta_i x - \alpha_i(\sin\beta_i x - \sinh\beta_i x)] \quad (13)$$

where $m = \rho_s A_s + 2\rho_p A_p$ is the mass per unit length of the beam, and α_i is expressed as

$$\alpha_i = \frac{\cos\beta_i L + \cosh\beta_i L}{\sin\beta_i L + \sinh\beta_i L} \quad (14)$$

The value β_i must satisfy the charactersistic equation given by

$$\begin{vmatrix} 1 & 0 & 1 & 0 \\ 0 & 1 & 0 & 1 \\ -\mathrm{c} & -\mathrm{s} & \mathrm{ch} & \mathrm{sh} \\ \begin{pmatrix} EI\beta^3\cdot\mathrm{s} \\ +A\cdot\mathrm{c} \end{pmatrix} & \begin{pmatrix} -EI\beta^3\cdot\mathrm{c} \\ +A\cdot\mathrm{s} \end{pmatrix} & \begin{pmatrix} EI\beta^3\cdot\mathrm{sh} \\ +A\cdot\mathrm{ch} \end{pmatrix} & \begin{pmatrix} EI\beta^3\cdot\mathrm{ch} \\ +A\cdot\mathrm{sh} \end{pmatrix} \end{vmatrix} = 0 \quad (15)$$

where c, s, ch, sh stand for $\cos\beta L$, $\sin\beta L$, $\cosh\beta L$, $\sinh\beta L$, and

$$A = \omega^2 k_e m_e / (k_e - \omega^2 m_e) \quad (16)$$

where $\omega = \beta^2\sqrt{EI/m}$ is the natural frequency of the Euler-Bernoulli beam. Consequently the explicit expression of the frequency equation can be obtained from Eq. (18) as

$$\begin{aligned}&(s+sh)[EI\beta^3(s-sh)+A(c-ch)]+\\&(c+ch)[EI\beta^3(c+ch)-A(s-sh)]=0\end{aligned} \quad (17)$$

Upon setting Eq. (8) into Eq. (7) and using the orthogonality conditions

$$\int_0^L m w_i(x) w_j(x) dx = \delta_{ij} \quad (18a)$$

$$\int_0^L (2E_p I_p + E_s I_s) w_i''(x) w_j''(x) dx = \delta_{ij}\omega_i^2 \quad (18b)$$

the Lagrangian equation can be rewritten as

$$\begin{aligned}L = {} & \frac{1}{2}\sum_{i=1}^{n}\dot{\eta}_i^2 + \frac{1}{2}mL\dot{z}^2 + m\int_0^L \dot{z}\sum_{i=1}^{n} w_i\dot{\eta}_i dx + \frac{1}{2}m_e(\dot{z}_0+\dot{z})^2 - \\ & \frac{1}{2}\sum_{i=1}^{n}\omega_i^2\eta_i^2 - \sum_{i=1}^{n}\vartheta_i\eta_i v + \frac{1}{4}C_p v^2 - \frac{1}{2}k_e(z_1-z_0)^2\end{aligned} \quad (19)$$

Next, the Lagrangian multipliers method [11] is used to derive the equations of motion for the energy harvesting system. The Lagrangian multipliers method states that, for a system described by a finite set of n generalized coordinat q_k $(k=1,\ldots,n)$ where m coordinates are not redundant, the system's equations of motion are

$$\frac{d}{dt}\left(\frac{\partial L}{\partial \dot{q}_k}\right) - \frac{\partial L}{\partial q_k} = Q_k + \sum_{l=1}^{m}\lambda_l\frac{\partial g_l}{\partial q_k} \qquad (k=1,\ldots,n) \quad (20)$$

where Q_k is the generalized force associated with the generalized variable q_k, λ_l is the l-th Lagrangian multiplier, and g_l is the l-th constraint equation. For the case here, n+3 generalized variables are used:

$$[q_1,\ldots,q_n,q_{n+1},q_{n+2},q_{n+3}] = [\eta_1,\ldots,\eta_n,z_0,z_1,v] \quad (21)$$

and only one constraint equation is considered:

$$g = w(L,t) - z_1(t) = \sum_{i=1}^{n} w_i(L)\eta_i(t) - z_1(t) = 0 \quad (i=1,\ldots,n) \quad (22)$$

By evaluating Eq. (19) in Eq. (20) and eliminating variables λ_1 and z_0, the following set of equations is obtained for the energy harvesting system:

$$\ddot{\eta}_i + \gamma_i\eta_i + 2\zeta_i\omega_i\dot{\eta}_i(t) + \chi_i v = \varphi_i\ddot{z} \quad (23a)$$

$$\frac{C_p}{2}\dot{v} + \frac{1}{R_l}v - \sum_{i=1}^{n}\vartheta_i\dot{\eta}_i = 0 \quad (23b)$$

where a modal damping ratio ζ_i is introduced to account for the structural damping due to the friction internal to the beam. The coefficients are expressed as

$$\gamma_i = \frac{\omega_i^2 + k_e(1-B)^2 w_i(L)^2}{1 + m_e B^2 w_i(L)^2} \quad (24a)$$

$$\chi_i = \frac{\vartheta_i}{1 + m_e B^2 w_i(L)^2} \quad (24b)$$

$$\varphi_i = \frac{\int_0^L m w_i dx + m_e B w_i(L)}{1 + m_e B^2 w_i(L)^2} \quad (24c)$$

$$B = \frac{A}{\omega^2 m_e} \quad (24d)$$

where R_l is the load resistor.

Assuming the beam undergoes a harmonic transverse base excitation as $z = Ze^{j\Omega t}$, the steady-state electromechanical responses should also be harmonic with the same frequency as $\eta_i = \mathrm{H}_i e^{j\Omega t}$ and $v = Ve^{j\Omega t}$. Substituting these terms into Eq. (23) and eliminating the term H_i, one can obtain the expression for the amplitude of voltage across the load resistance as

$$V = -\frac{\sum_{i=1}^{\infty}\dfrac{j\Omega^3\vartheta_i\varphi_i Z}{\gamma - \Omega^2 + 2j\Omega\omega_i\zeta}}{\dfrac{1}{R_l} + j\omega\dfrac{C_p}{2} + \sum_{i=1}^{\infty}\dfrac{j\Omega\vartheta_i}{\gamma - \Omega^2 + 2j\Omega\omega_i\zeta}} \quad (25)$$

The resulting voltage amplitude can then be used in $v = Ve^{j\omega t}$ to get the steady-state voltage response under a harmonic base excitation. Meanwhile, one can easily obtain the current generated by the PZT by using $i(t) = v(t)/R_l$, as well as the instantaneous power output according to the well-known relation $P(t) = v(t)^2/R_l$. In addition, it is possible to solve Eq. (23) for the amplitude of the modal mechanical response as

$$\begin{aligned}\mathrm{H}_i = {} & \frac{\Omega^2 Z}{\gamma - \Omega^2 + 2j\Omega\omega_i\zeta}\times \\ & \left(\frac{\sum_{i=1}^{\infty}\dfrac{j\Omega^3\vartheta_i\varphi_i Z}{\gamma - \Omega^2 + 2j\Omega\omega_i\zeta}}{\dfrac{1}{R_l} + j\omega\dfrac{C_p}{2} + \sum_{i=1}^{\infty}\dfrac{j\Omega\vartheta_i}{\gamma - \Omega^2 + 2j\Omega\omega_i\zeta}} - \varphi_i\right)\end{aligned} \quad (26)$$

and solve Eq. (12) for the amplitude of the mass as

$$Z_0 = \sum_{i=1}^{\infty}\frac{k_e w_i(L)\mathrm{H}_i}{(k_e - \Omega^2 m_e)} \quad (27)$$

Subsequently, the steady-state mechanical responses of the relative displacement of the beam and the mass can be obtained using $w(x,t) = \sum_{i=1}^{\infty} w_i \mathrm{H}_i e^{j\Omega t}$ and $z_0 = Z_0 e^{j\Omega t}$, respectively.

PARAMETRIC STUDY

A parametric case study is carried out in this section. The geometric and material parameters of the bimorph are given in

Table 1. Note that the material parameters in Table 1 are also available from [12].

Table 1. Geometric and material parameters of the sample PEH

Beam length L (mm)	50
Beam width b (mm)	5
Thickness of piezoelectric layer h_p (mm)	0.15
Thickness of substructure layer h_s (mm)	0.1
Mass density of substructure layer ρ_s (kg/m^3)	7165
Mass density of piezoelectric layer ρ_p (kg/m^3)	7800
Young's modulus of substructure layer E_s (GPa)	100
Young's modulus of piezoelectric layer c_{11}^E (Gpa)	66
Piezoelectric coupling coefficient e_{31} (pm/V)	-190
Permittivity at constant stress ε_{33}^S (nF/m)	15.93
Damping ratio of 1st mode ζ_1	0.01
Load resistance R_l (Ohm)	10^6

In the following discussion, a series connection of the PZT layers is used. The PZT layers are assumed to be identical and their conductive electrodes are assumed to be fully covering the respective surfaces of the PZT layers at the top and bottom. The excitation of the PEH comes from the harmonic base vibration in the transverse direction only. Note that the fundamental mode is of major interest in energy harvesting problems, because in most cases the maximum electrical response occurs in the fundamental mode. Therefore, the following parametric study discusses the electromechanical responses of the PEH at the fundamental mode. The frequency-response curves (FRCs) of the electro-mechanical outputs are plotted, and the effects of the mass and the stiffness on the frequency responses are investigated.

1) VARIATION OF EIGENFREQUENCIES

The system's natural frequencies are related to the dimensionless frequency parameters $\hat{\beta}_i = \beta_i L$, which are the roots of the frequency equation Eq. (17). Based on the beam's geometric and material properties in Table 1, the effects of the spring-mass system on the first three eigenfrequencies, $\omega_{1,2,3} = \hat{\beta}_{1,2,3}^2 \sqrt{EI/(mL^4)}$, of the primary system are shown in Table 2. It can be seen that, when the value of the mass is maintained, enlarging the spring stiffness tends to increase the eigenfrequencies. Nevertheless, when the spring stiffness is unchanged, increasing the mass value generally decreases the eigenfrequencies. By properly choosing and combining the mass and the spring stiffness, the natural frequency of the system will be altered. This provides a possibility of tuning the energy harvester's working frequency to match a certain frequency of ambient vibrations. Besides the frequency-tuning advantage, adding the spring-mass system will also enlarge the vibration amplitude as well as the voltage/power output of the energy harvester at low frequency levels, as will be discussed in the next section.

Table 2. Effects of the spring and mass on $\omega_{1,2,3}$ of the system (ω_i in Hz, k_e in N/m, m_e in g)

k_e \ m_e	0.5	1	2	4
20	25.8159	18.4362	13.0982	9.2833
	94.0192	93.0942	92.6554	92.4419
	483.9250	483.9190	483.9159	483.9144
50	32.4718	23.5964	16.9095	12.0358
	116.9615	113.8213	112.3158	111.5806
	488.2088	488.1705	488.1515	488.1420
100	35.8504	26.4603	19.1226	13.6707
	147.1805	141.0500	138.0302	136.5364
	495.6292	495.4743	495.3980	495.3601
500	39.1521	29.5283	21.6241	15.5727
	259.1831	244.5450	236.8482	232.9056
	563.5485	560.0719	558.4055	557.5899

2) FREQUENCY RESPONSE OF THE ELECTRICAL OUTPUT

The voltage frequency response function in the fundamental mode is described as the ratio of the voltage output to the base acceleration as

$$\frac{V}{\Omega^2 Z e^{j\Omega t}} = -\frac{\dfrac{j\Omega \vartheta_1 \varphi_1}{\gamma - \Omega^2 + 2j\Omega\omega_1\zeta}}{\dfrac{1}{R_l} + j\omega\dfrac{C_p}{2} + \dfrac{j\Omega\vartheta_1}{\gamma - \Omega^2 + 2j\Omega\omega_1\zeta}} \tag{28}$$

To analyze the effect of the spring stiffness on the voltage output, different values of the spring stiffness are chosen while the mass is set to remain unchanged at 0.002 kg. Fig. 2 shows the FRC of the voltage output across a 1MOhm load resistance when different spring stiffness are used. It can be seen from Fig. 2 that, after adding the tip spring-mass system, two resonance frequencies appear in the voltage FRC. The amplitude of the voltage response at the first resonant frequency is larger than that at the second resonant frequency, and both amplitudes at the first and second resonant frequencies can be larger than that of a single bimorph without spring mass system, depending on the value of the spring stiffness. Meanwhile, larger spring stiffness tends to results in higher resonant frequency and lower corresponding voltage amplitude. It is also worth noticing that, at the lower frequency level, the voltage generated from the system with spring-mass attached is much greater than that without the spring-mass attachment. This indicates that the spring-mass system can be properly used to not only tune the operating frequency of a bimorph PEH, but also greatly improve the voltage-generating ability at a low frequency level, making it useful for low-frequency applications.

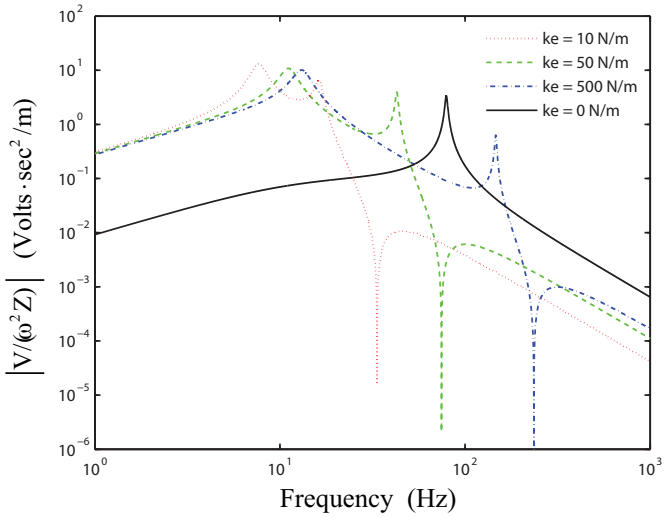

Figure 2. Effects of the spring stiffness on the voltage frequency response (m_e =0.002kg)

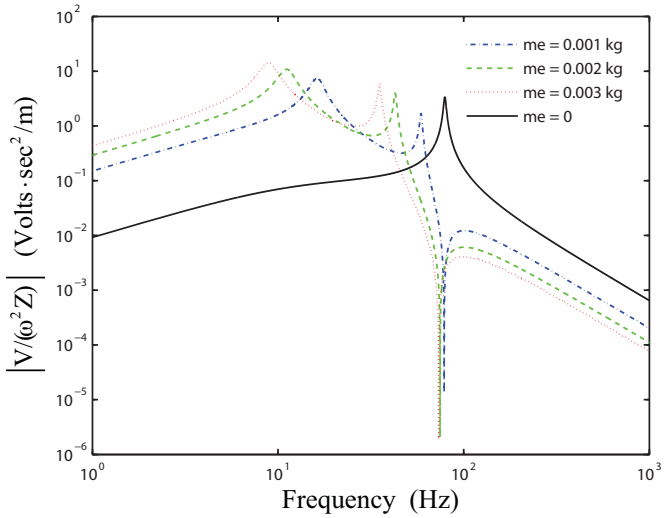

Figure 3. Effects of the mass on the voltage frequency response (k_e =50N/m)

Fig. 3 shows the effects of the mass on the voltage frequency response, in which the spring stiffness is fixed to 50 N/m and the load resistor is 1MOhm. It can be seen that increasing the mass tends to reduce the resonant frequency whereas enlarge the amplitude of voltage output. Meanwhile, the voltage amplitude diminishes at the frequency close to the resonant frequency of a single bimorph. Compared to the voltage FRC in Fig. 2 where increasing the spring stiffness barely changes the voltage output below the first resonant frequency, Fig. 3 shows that increasing the mass largely increases the voltage at a low frequency range. In addition, both Fig. 2 and Fig. 3 show that adding the spring-mass system will decrease the amplitude of voltage at frequencies greater than the resonant frequency of a single bimorph.

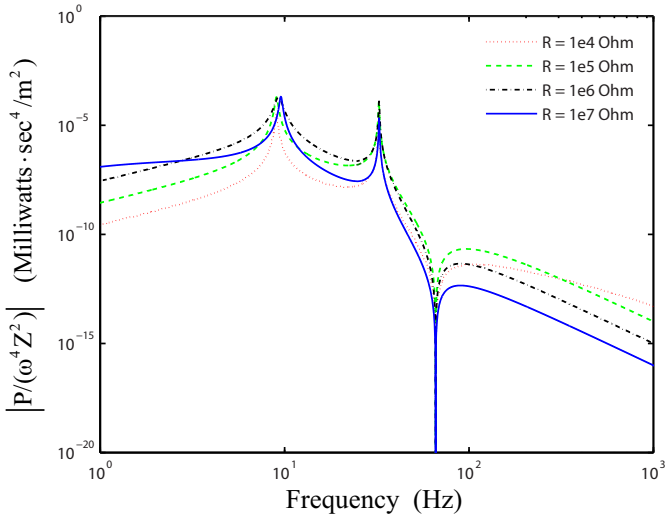

Figure 4. Effects of the load resistance on the power frequency response (k_e =50N/m, m_e =0.002kg)

The power frequency response function is written as the ratio of the power output to the square of the base acceleration:

$$\frac{P}{\Omega^4 Z^2 e^{j2\Omega t}} = -\frac{(\frac{j\Omega\vartheta_1\varphi_1}{\gamma-\Omega^2+2j\Omega\omega_1\zeta})^2}{R_l(\frac{1}{R_l}+j\omega\frac{C_p}{2}+\frac{j\Omega\vartheta_1}{\gamma-\Omega^2+2j\Omega\omega_1\zeta})^2} \quad (29)$$

As the power FRC is similar to the voltage FRC, the effects of the spring-mass system on the power FRC is not plotted here. Nevertheless, as the load resistance plays an important role in determining the total output power, the effects of load resistance on the power FRC is shown in Fig. 5, in which a 50N/m spring stiffness and a 0.002kg mass are used. It can be observed from Fig. 5 that the power FRC does not change monotonically with the changing load resistance. This corresponds to the power FRC of a single cantilevered PEH [12]. The largest power output can be achieved when the load resistance is around 10^7 Ohm. Moreover, an optimal load resistance can be obtained by differentiating Eq. (31) with respect to R_l and solving for R_l after setting the differentiated equation to 0.

3) FREQUENCY RESPONSE OF THE MECHANICAL OUTPUT

The frequency response of the beam's relative tip motion is defined as the ratio of the relative tip displacement amplitude to the amplitude of the base excitation:

$$\frac{W}{\Omega^2 Z e^{j\Omega t}} = \frac{w_1(L)}{\gamma-\Omega^2+2j\Omega\omega_i\zeta}\times \left(\frac{\frac{j\Omega\vartheta_1\varphi_1\chi_1}{\gamma-\Omega^2+2j\Omega\omega_1\zeta}}{\frac{1}{R_l}+j\omega\frac{C_p}{2}+\frac{j\Omega\vartheta_1}{\gamma-\Omega^2+2j\Omega\omega_1\zeta}}-\varphi_1\right) \quad (30)$$

Fig. 5 shows the effects of the spring stiffness on the FRC of the relative tip displacement of the beam. After adding the spring-mass system, two resonance frequencies that are smaller than the resonant frequency of a single bimorph are observed in the tip motion FRC. Similar to the voltage FRC in Fig. 2, one can observe from Fig. 5 that increasing the spring stiffness tends to increase the first and second resonant frequencies, however, decrease the tip displacement amplitude. Also can be seen from Fig. 5 is that, for the system with a spring-mass attachment, the tip motion at its first resonant frequency is larger than the maximum tip motion of a single bimorph. The tip motion at the second resonant frequency can be greater than the tip motion of a single bimorph when the spring stiffness is smaller than 50N/m. Furthermore, Fig. 6 shows the effects of the mass on the beam's tip motion. Again, one can observe that a heavier mass causes a larger tip displacement but smaller resonant frequencies.

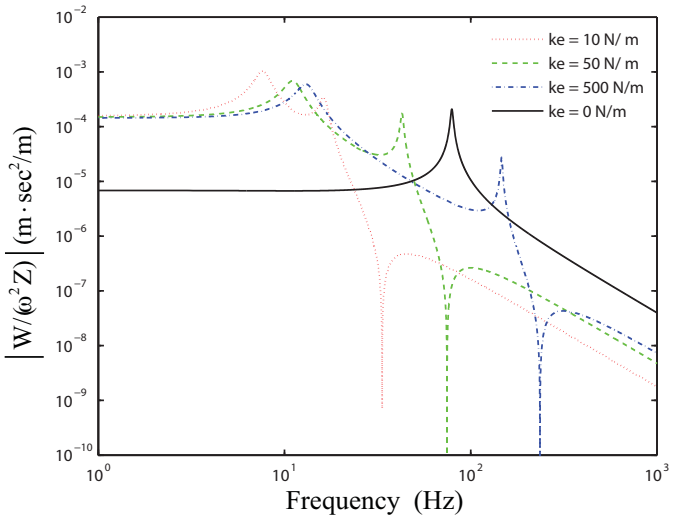

Figure 5. Effects of the spring stiffness on the relative tip displacement of the beam (m_e =0.002kg)

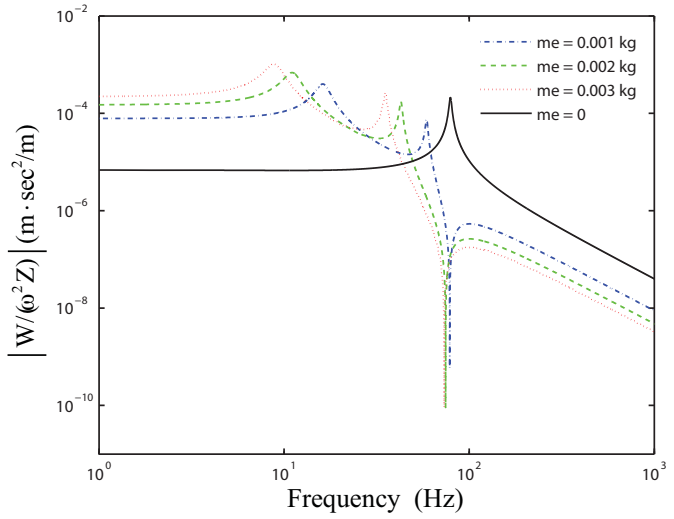

Figure 6. Effects of the mass on the relative tip displacement of the beam (k_e =50N/m)

CONCLUSIONS

This paper presents the modeling and analysis of a frequency-tunable piezoelectric energy harvester (PEH) that consists of a bimorph and a tip spring-mass system. An electromechanical model of the proposed harvester is derived based on the Lagrange multipliers method. The model is used in a harmonic base excitation case study. Frequency responses of the electromechanical outputs show that the proposed PEH is able to be tuned to work efficiently at two resonance frequencies, and can generate more voltage and power as compared to a bimorph without the spring mass system by properly selecting the mass and the spring stiffness.

ACKNOWLEDGMENTS

The authors would like to acknowledge the Natural Sciences and Engineering Research Council of Canada for providing the funding for this research.

REFERENCES

[1] Anton, S.R. and Sodano H.A., 2007, "A review of power harvesting using piezoelectric materials 2003-2006" Smart Mater. Struct., Vol 16, R1–21

[2] IEEE, 1987, *Standard on Piezoelectricity*, IEEE, New York.

[3] Zhu D., Tudor M.J. and Beeby S.P., 2010, "*Strategies for increasing the operating frequency range of vibration energy harvesters: a review*", Meas. Sci. Technol., Vol. 21, 022001

[4] Roundy S., 2005, "*On the effectiveness of vibration-based energy harvesting*", J. Intell. Mater. Sys. Struct., Vol. 16, No. 10, 809-823

[5] Shen D., Park J., Ajitsaria J., Choe S., Wikle III H.C. and Kim D., 2008, "*The design, fabrication and evaluation of a MEMS PZT cantilever with an integrated Si proof mass for vibration energy harvesting*" J. Micromech. Microeng., Vol. 18, 055017

[6] Roundy S., Leland E.S., Baker, J., Carleton, E., Reilly, E., Lai E., Otis B., Rabaey, J.M., Wright, P.K. and Sundararajan, V., 2005, "*Improving power output for vibration-based energy scavengers*", IEEE Pervasive Computing, Vol. 4, pp 28-36

[7] Challa V.R., Prasad M.G., Shi Y. and Fisher F.T., 2008, "*A vibration energy harvesting device with bidirectional resonance frequency tunability*", Smart Mater. Struct., Vol. 17, 015035

[8] Wu W.J., Chen Y.Y., Lee B.S., He J.J. and Peng Y.T., 2006, "*Tunable resonant frequency power harvesting devices*", Proc. SPIE, Vol. 6169, pp 55–62

[9] Hu Y., Xue H. and Hu H., 2007, "*A piezoelectric power harvester with adjustable frequency through axial preloads*", Smart Mater. Struct., Vol. 16, 1961

[10] Rao, S.S., 2005, *Mechanical Vibrations Fourth Edition in SI Units*, Prentice Hall, Singapore
[11] Preumont A., 2003, *Mechatronics: Dynamics of Electro-mechanical and Piezoelectric Systems*, Springer, The Netherlands
[12] Erturk A. and Inman D.J., 2008, "A Distributed Parameter Electromechanical Model for Cantilevered Piezoelectric Energy Harvesters", J. Vib. Acoust., Vol. 130, 041002